Brazilian Journal
of Chemical
Engineering

ISSN 0104-6632
Printed in Brazil
www.abeq.org.br/bjche

Vol. 33, No. 03, pp. 661 - 673, July - September, 2016
dx.doi.org/10.1590/0104-6632.20160333s20150137

NANOBIOCATALYTIC SYSTEMS BASED ON LIPASE-Fe_3O_4 AND CONVENTIONAL SYSTEMS FOR ISONIAZID SYNTHESIS: A COMPARATIVE STUDY

V. M. Costa[1], M. C. M. de Souza[2], P. B. A. Fechine[1], A. C. Macedo[2*] and L. R. B. Gonçalves[2]

[1]Grupo de Química de Materiais Avançados, (GQMAT), Departamento de Química Analítica e Físico-Química, Universidade Federal do Ceará, UFC, Campus do Pici, C.P. 12100, CEP: 60451-970, Fortaleza - CE, Brazil.
[2]Grupo de Pesquisa em Desenvolvimento de Processos Biotecnológicos, (GPbio), Departamento de Engenharia Química, Universidade Federal do Ceará, UFC, Campus do Pici, CEP: 60455-760. Fortaleza - CE, Brazil.
E-mail: acasimiro@gmail.com

(Submitted: February 28, 2015 ; Revised: October 16, 2015 ; Accepted: October 19, 2015)

Abstract - Superparamagnetic nanomaterials have attracted interest in many areas due to the high saturation magnetization and surface area. For enzyme immobilization, these properties favor the enzyme-support contact during the immobilization reaction and easy separation from the reaction mixture by use of low-cost magnetic processes. Iron oxide magnetic nanoparticles (Fe_3O_4, MNPs), produced by the co-precipitation method, functionalized with 3–aminopropyltriethoxysilane (APTES) and glutaraldehyde (GLU), were evaluated as a solid support for *Candida antarctica* lipase B (CALB) immobilization. The nanomagnetic derivative (11nm) obtained after CALB immobilization (MNPs/APTES/GLU/CALB) was evaluated as biocatalyst in isoniazide (INH) synthesis using ethyl isonicotinate (INE) and hydrazine hydrate (HID) as substrates, in 1,4-dioxane. The results showed that MNPs/APTES/CALB had a similar performance when compared to a commercial enzyme Novozym 435, showing significant advantages over other biocatalysts, such as *Rhizhomucor miehei* lipase (RML) and CALB immobilized on non-conventional, low-cost, chitosan-based supports.
Keywords: Isoniazid; Magnetic Nanoparticles; Nanobiocatalytic systems; Lipase; Tuberculostatic Drug.

INTRODUCTION

Tuberculosis (TB) is an infectious disease caused by *Mycobacterium tuberculosis* that produces several million deaths annually worldwide. According to the World Health Organization, in 2013, an estimated 9.0 million people developed TB and 1.5 million died from the disease (WHO Global Tuberculosis Report 2014). Isoniazid (INH) is the most frequently prescribed antibiotic in the treatment of tuberculosis. INH has a greater efficacy and acceptable toxicity and thus belongs to the first-line drugs group for TB treatment, while the second-line ones like kanamycin, amikacin, capreomycin, cycloserine, ethionamide, para-aminosalicylic acid and fluoroquinolones show a lower efficacy or a greater toxicity in TB treatment (Barry, 1997; Vavříková *et al*. 2011; Matei *et al*., 2013).

Chemically INH is an isonicotinic acid hydrazide ($C_6H_7N_3O$), first synthesized in 1912. At present, the synthesis of INH is carried out by the chemical process using 4-cyanopyridine and hydrazine hydrate as reactants in the presence of sodium hydroxide at 100 ºC under reflux conditions for 7 h (Yadav *et al*., 2004; Sittig, 1998; Gogte, 1982). This conventional

*To whom correspondence should be addressed
This is an extended version of the work presented at the 20th Brazilian Congress of Chemical Engineering, COBEQ-2014, Florianópolis, Brazil.

chemical pathway for INH synthesis has a yield of 62% (INH mass). Due to the use of 4-cyanopyridine as reactant and intensive heat, this chemical route is hazardous and expensive. In contrast, biocatalyzed reactions using enzymes are conducted at milder temperature, attractive particularly for chemical and drug synthesis in aqueous and non-aqueous media. In particular, microbial lipases or triacylglycerol hydrolases (E.C. 3.1.1.3) have wide industrial applications in organic synthesis as environmentally friendly catalysts (Yadav and Sajgure, 2007; Yadav *et al*., 2004).

Lipases are applicable for catalysis of esterification and transesterification reactions in non-aqueous media via an acyl-enzyme intermediate formation mechanism (Akoh *et al*., 2007; Al-Zuhair *et al*., 2007; Abbas and Comeau, 2003; Björkling *et al*., 1991; Brzozowsky *et al*., 1991; Hæffner *et al*., 1998). However, unusual reactions such as aminolysis, used for INH synthesis, may also be catalyzed by lipases. Gotor *et al*. (1991) and Gotor-Fernández *et al*. (2006) described the aminolysis and transamidation reactions catalyzed by lipases. Recently, Yadav *et al*. (2004), based on the Gotor *et al*. studies, described the reaction of ethyl isonicotinate with hydrazine hydrate as a nucleophile carried out in 1,4-dioxane as solvent to produce INH with lipases via the reaction mechanism described in Figure 1.

As shown in Figure 1, in the chemical mechanism for isoniazid synthesis in the catalytic lipase site, the first step is the acyl-enzyme complex formation that starts with ethyl isonicotinate. A tetrahedral intermediate formation step occurs after ethyl isonicotinate addition. The formation of the acyl-enzyme complex occurs when ethanol is released and the second stage starts with the participation of the second substrate, hydrazine hydrate. Hydrazine hydrate acts as the nucleophile, reacting with the acyl-enzyme complex to form another tetrahedral intermediate. A final deacylation step results in isoniazid formation and its subsequent release. This mechanism has been the subject of several studies such as Brzozowsky *et al*. (1991) and Haeffner Norin (1999).

Despite the great potential of lipases, the low thermal and mechanical stability and difficulties in recovery and enzyme re-use are limitations in free enzyme use. A wide variety of immobilization techniques may be employed in order to reduce these operational problems and improve the catalytic activity and ability of these enzymes. It is possible to vary the nature of the immobilized derivative in order to design efficient biocatalytic processes (Adriano *et al*., 2005; Mohy Eldin *et al*., 2000).

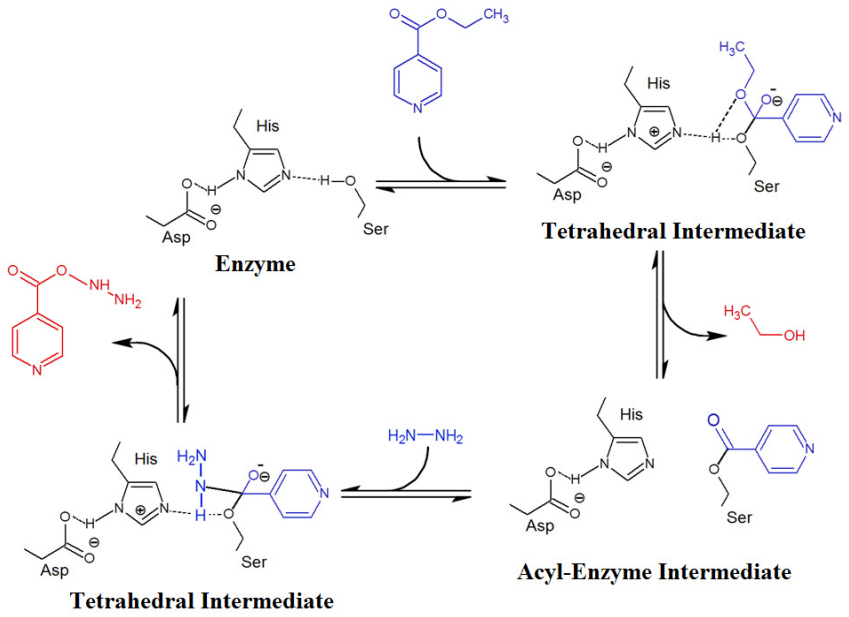

Figure 1: Isoniazid synthesis reaction biocatalyzed using Lipases (chemical mechanism).

In recent years, considerable attention has been devoted to the use of nanostructured materials as enzyme immobilization supports. In this context, the nanostructures emerge as new alternative supports, enabling new properties such as high surface area, high temperature tolerance, high chemical reactivity and high enzymes-substrate interactions. Among the nanostructured materials employed in enzyme immobilization techniques, modified magnetic iron nanoparticles (MNPs) are an attractive approach for enzyme stabilization due to facile recovery at the end of their use by magnetic processes. The outstanding potential of these iron oxide nanobiocatalysts in bioprocesses for production of fuels, chemicals and pharmaceuticals has stimulated the extensive development of synthetic technology to obtain nanobiocatalysts with industrial applications and social-economic advantages. Therefore, many technologies, such as co-precipitation, microemulsion, thermal decomposition and hydrothermal synthesis have been applied and reviewed for the production of the MNPs. However, as is well known, co-precipitation is one of the most diffused and low-cost techniques due to its simplicity as an efficient chemical pathway for the preparation of various interesting solid-state materials. Fe^{+2} and Fe^{+3} salts precursors are mixed in solution with the addition of a weak base to cause precipitation of the nanoparticles to form a good crystalline phase. It is possible to control the form (size and homogeneity) and structure (morphology) to obtain different shapes (microspheres, nanospheres, nanorods and ferrofluids) and sizes for MNPs (Adachi *et al*., 2004; Young *et al*., 2008; Law *et al*., 2009; Jang *et al*., 2010; Barreto *et al*., 2011).

This paper aims to report a synthesis of a novel magnetic nanosystem based in superparamagnetic nanoparticles of Fe_3O_4 and lipase B from *Candida antarctica* (CALB) and its evaluation in INH synthesis. A comparative performance study of low-cost conventional catalysts is presented in order to investigate the feasibility of applying these MNPs-CALB in industrial processes as an alternative to commercial systems already studied by Yadav *et al*. (2004).

MATERIAL AND METHODS

MNPs-CALB Synthesis (Biocatalyst Synthesis)

The MNPs synthesis followed Barreto *et al*. (2011) methodology. For the co-precipitation, a solution of metal salts containing Fe^{+2} and Fe^{+3} ($FeSO_4.7H_2O$ and $FeCl_3.6H_2O$ 1:2) was mixed and diluted in milli-Q water to form the spinel phase (Fe_3O_4). The aqueous mixture was heated to 70 °C under constant stirring and 30 wt% NH_4OH solution added to pH 10 for the formation of a black precipitate (1).

$$Fe^{+2} + 2Fe^{+3} + 8OH^- \rightarrow Fe_3O_4 + 4H_2O \quad (1)$$

The precipitate was washed for several times with milli-Q water until the residual solution reached neutral pH and a single washing with methanol. The sample of magnetic nanoparticles was dryed in a desiccator under vacuum. The functionalization of magnetite using 3–aminopropyltriethoxysilane (APTES) was performed following the modified methodology of Can *et al*. (2009). In a round bottom flask, a suspension of 100 mg of magnetite was preprared in a mixture of ethanol and toluene in a 1:2 ratio. Mass proportions of magnetite and APTES at the ratios (1:1), (1:2) and (1:3) were reacted under an inert atmosphere with constant stirring for 24 h until the color changed to a brown solid, according to Figure 2(A). The separated precipitate was washed several times with ethanol until complete removal of residues and dried in a desiccator under constant vacuum. After treatment with APTES, activation was performed in a solution of 0.6% (v/v) glutaraldehyde for 2 h at 25 °C (according to Figure 2(B). After this step, the nanoparticles were washed with 100 mM sodium carbonate-bicarbonate buffer, pH 7.0, to remove the excess activator agent. CALB immobilization was carried out by added 0.01 g of nanoparticles (treated with APTES and glutaraldehyde cross-linked) with 0.5 ml of 100 mM buffer solution of sodium bicarbonate, pH 7.0. The system was kept under controlled stirring: 20-250 rpm (orbital shaking); the contact time between enzyme-support was 1 h, leading to the immobilized enzyme according to Figure 2(C). Immobilization yield (%) was calculated by measuring the initial (At_i) and the final (At_f) enzyme activity in the supernatant and in the blank assay, according to Silva *et al*. (2012):

$$IY_{imob}(\%) = \frac{At_i - At_f}{At_i} * 100 \quad (2)$$

MNPs and MNPs-CALB Characterization (Biocatalyst Characterization)

X-ray Diffraction (XRD) was performed on a Rigaku X-ray powder diffractometer with CuKα (λ = 1.54056 Å) operating at 40 kV/25mA. To perform the analysis, the powder samples were accommodated in the sample holder and the diffraction patterns were collected over a range of 2θ= 20-100° with 0.02° step. Additionally, the values of particle

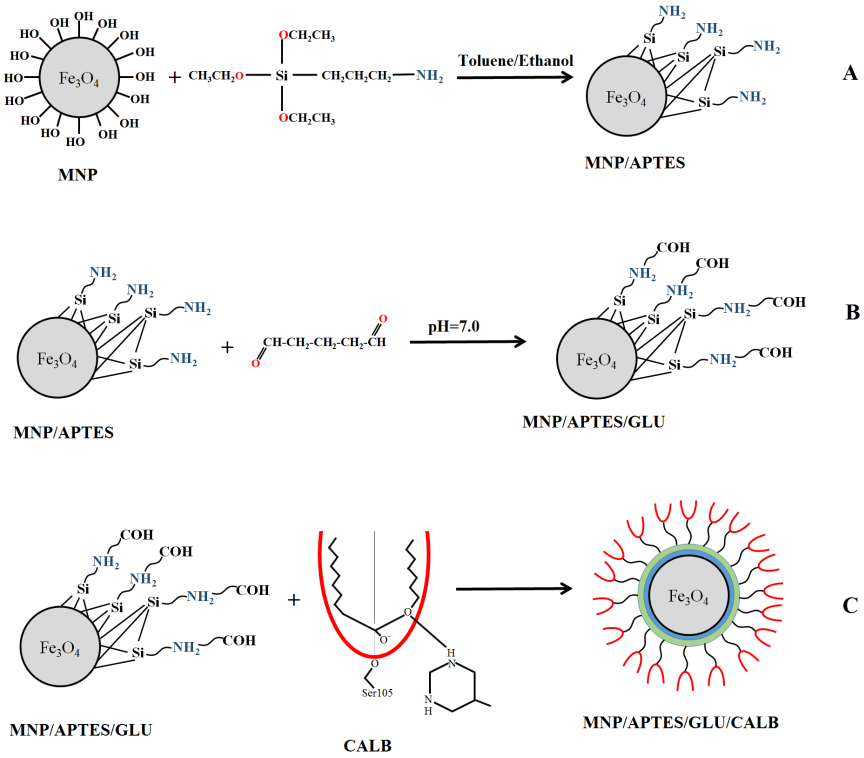

Figure 2: (A) Magnetic nanoparticle (MNPs) functionalization with 3-aminopropyl triethoxysilane (APTES) in toluene and ethanol, **(B)** Glutaraldehyde (GLU) reticulation of MNPs after APTES treatment, **(C)** *Candida antarctica Lipase B* (CALB) Immobilization on APTES functionalized MNPs after GLU reticulation.

size, lattice parameters and phase concentrations were calculated from the mathematical treatment of the diffraction patterns obtained by refining of the crystalline material using the *Rietveld Method*.

Infrared Spectroscopy (FTIR) data were obtained on a Perkin Elmer FTIR Spectrometer instrument. To perform the measurements, the samples were diluted in KBr and the spectra collected (400-4000 cm^{-1}).

Magnetic Measurements were obtained at room temperature using a vibrating sample magnetometer calibrated using a pure Ni wire. Measuring the mass of each sample the magnetic properties were evaluated and the results shown in emu/g. The range of the (opposite direction) magnetic field was -10.000 Oe to 10.000 Oe (Oersted), in order to understand the magnetic response of the sample.

Lipase Immobilization on Chitosan and Octyl-Silica

In order to compare the performance of the MNPs-CALB with other biocatalysts, lipases were immobilized on chitosan and octyl-silica. The immobilized enzymes, prepared according to protocols developed by *Grupo de Pesquisa e Desenvolvimento de Processos Biotecnológicos (GPBIO)*, were: *Rhizhomucor miehei* lipase supported on chitosan (CHI/RML), CALB supported on chitosan (CHI/CALB), described by Honorato *et al*. (2013) for INH synthesis, and CALB supported on Octyl-silica (OCSIL/CALB) derivatives, described by Lima de Matos (2014).

Preparation of CHI/RML and CHI/CALB

Powdered chitosan was dissolved in an acetic acid 5% ($v.v^{-1}$) solution. The obtained solution of 2.5% ($m.v^{-1}$) was dropped into a gently stirred 100mM NaOH solution at 25 °C (ratio chitosan/NaOH 1:10). After 24 h, chitosan beads were washed exhaustively with distilled water until neutrality and then dried by vacuum filtration. Chitosan beads were crosslinked in 100 mM sodium phosphate buffer solution, pH 7.0, containing 0.6% ($v.v^{-1}$) glutaraldehyde (ratio V_{gel}/V_{total} 1:10) for 60 min at 25 °C under slow stirring. After that, the chitosan support was washed thoroughly with distilled water to remove excess glutaraldehyde and then dried under vacuum. After that, the support and the enzymes were incubated in the presence of surfactants under slow stirring for 5 h at 25 °C. Afterwards, the immobilized enzyme was washed several times with distilled water to remove the excess of surfactant and glutaraldehyde and stored at 4 °C.

Preparation of OCSIL/CALB

Initially, silica was protonated by immersion in hydrochloric acid solution (0.1 M) for 1 h (under stirring). Subsequently, protonated silica was dried at 200 °C (5 h).

The silanization process was based on the methodology used by Tani and Suzuki (1996). After the acid treatment, the activation of the silica with octyl groups consisted in preparing a suspension containing 1 g of treated dry silica, 20 ml of a mixture of toluene/octyl(triethoxy)silane in the volume ratio 1:10. This suspension was refluxed for 3 h (82 °C). After the activation period, the support was filtered and washed with toluene, methanol and distilled water. At the process end, drying (room temperature) of the support was performed.

The immobilization step consisted, initially, in preparing a support suspension containing sodium phosphate buffer (100 mM, pH 7, room temperature) in the ratio of 10 ml buffer for each 0.5 g of support. The enzymatic load was 16 UpNPB.g^{-1} support. After the immobilization step, the solution was filtered and the solid was separated.

Hydrolytic Activity Analysis

Hydrolytic activity was assessed via colorimetric analysis using *p*-nitro-phenylbutyrate (*p*NPB). *p*NPB enzymatic hydrolysis was measured by UV-vis at 410 nm wavelength. One activity unit (1 U) corresponds to the amount of enzyme that hydrolyzes 1 mmol *p*NPB per minute at pH 7.0 and 25 °C (Kordel *et al*., 1991). In this work, the activity of the immobilized enzyme (Derivative activity: At_d - U/g support) was also measured by *p*NPB hydrolysis.

Isoniazide (INH) Synthesis: Reaction Characterization

The experimental set up consisted of mechanically agitated flasks, which were maintained at the desired temperature. The reaction mixture consisted of 0.4 mol of ethyl isonicotinate (Merck) and 1 mol hydrazine hydrate (Merck) diluted to 30 mL with 1,4-dioxane (Merck) as solvent. The reaction mixture was agitated at 30 ºC for 20 min at a speed of 150 rpm and 50 mg of immobilized enzyme was added to initiate the reaction. Supernatant liquid samples were withdrawn periodically and analyzed by HPLC coupled to a UV detector (set at 273 nm), using a Merck 50938® column with a stationary phase of Lichrosphere 100 RP-18 (particle size 5 µm), prepacked in a 250 mm × 4 mm column, and methanol:water (70:30) as mobile phase at 0.8 mL/min. The HPLC retention times for INH and isonicotinic acid ethyl ester were 4.61 and 2.56 min, respectively.

Different immobilized lipases were evaluated, MNPs-CALB, CHI/RML, CHI/CALB OCSIL/CALB and Novozym 435. CALB immobilized on a macroporous polyacrylic resin was used as a commercial standard for comparative study.

Hydrazinolytic Activity Analysis

Hydrazinolytic activity (HA) analyses were performed to understand the INH synthesis performance. This analysis was conducted at neutral pH (pH=7, 25 °C) and substrate concentrations of 0.4 mol of ethyl isonicotinate (Merck) and 1 mol hydrazine hydrate (Merck) diluted to 30 mL with 1,4-dioxane (Merck). One unit (1 U) of *hydrazinolytic activity* was defined as the amount of enzyme that consumes 1 µmol of ethyl isonicotinate with formation of isoniazid per min at pH 7 and 25 °C.

Thermal Stabilities of Soluble and Immobilized CALB

Soluble or immobilized CALB was incubated in 100 mM sodium phosphate buffer, pH 8.0, at 60 °C, for 21h. Periodically, samples were withdrawn and their residual activities were assayed by the hydrolysis of *p*-nitrophenyl butirate, previously described. The initial activity was taken as 100%. The deactivation constant and half-life ($t_{1/2}$) for each immobilized derivative were calculated according to the Sadana and Henley model (Sadana and Henley, 1987; Sadana, 1988). With the exponential nonlinear decay model and its parameters, it was possible to determine the inactivation constant (kd) and the half-lives ($t_{1/2}$) of the derivatives. Stabilization factors were obtained as the ratio between half-lives of the derivatives and the soluble CALB.

RESULTS AND DISCUSSION

Biocatalyst Synthesis

CALB was covalently immobilized on the APTES-modified Fe_3O_4 nanoparticles by forming a Schiff base linkage between the aldehyde group (glutaraldehyde) and the enzyme terminal amino group. Various factors can affect the immobilization interactions, including stirring speed, enzyme load, enzyme-support contact time and APTES proportion used to modify the Fe_3O_4 nanoparticle surface. In this study, these

various factors that affect the CALB immobilization on the Fe3O4 nanoparticles were evaluated to determine their influence on the immobilization efficiency (yield) and the derivative activity recovery.

Effect of the Stirring Speed on the CALB Immobilization

The effect of the stirring speed on the immobilization of the enzyme on MNPs is shown in Figure 3(A). The type of stirring (orbital or rotational) was also analyzed. Due to equipment limitations, the influence of rotational stirring was investigated at 20 and 45 rpm. Speeds from 20 to 250 rpm were investigated using orbital stirring. In both cases, the system was stirred for 1 h. When the orbital stirring was used in the range between 20-180 rpm, no significant variations were observed in the derivative activity. A decrease in derivative activity was observed when the stirring speed was enhanced to 250 rpm. Regarding rotational stirring, in which shear forces are prevalent, derivative activity enhanced when the stirring speed was increased from 20 to 45 rpm. The shear agitation improves contact and interactions between the enzyme and support, creating a better condition for enzyme immobilization (Kaya *et al*., 1994; Kim *et al*., 2006; Mozhaev and Martinek, 1982). In fact, the best derivative activity (17.5 ± 0.5 U.g^{-1}) was observed when rotational stirring at 45 rpm was used. However, an excessive increase in shear rate may promote a reduction in the enzyme-support binding, probably due to enzyme denaturing caused by shear forces excessively applied. Although no experiment was carried out with rotational stirring above 45 rpm, it is possible to deduce that the excessive action of forces generated by agitation may promote a decrease in derivative activity. The enzyme denaturation phenomenon was also observed at 250 rpm (orbital stirring). Therefore, based on these results, all further experiments were conducted at 45 rpm and rotational stirring.

Effect of the Enzyme Load

The effect of enzyme load was conducted from 45 to 200 U.g^{-1} (At_t). As shown in Figure 3(B), when the enzyme load was increased to 80 U.g^{-1} support, an increase in derivative activity was observed. The increase in enzyme load allows a larger available enzyme amount for enzyme-support interactions, increasing the support surface coating. In fact, this phenomenon was evidenced by the highest derivative activity value (29.1 U. g^{-1} ± 0.9) achieved for 80 U. g^{-1} support of enzyme load. The increase in enzyme load also causes an increase in the protein-protein interactions, which promotes the possible formation of multiple enzyme layers, also creating a barrier to product and substrate diffusion (Silva *et al*., 2012). This diffusional limitation behavior was observed when 200 U.g^{-1} (At_t) was used. Regarding immobilization yield, it is possible to observe that the increase in enzyme load causes an immobilization yield reduction. Similar behavior was reported by Xie and Ma (2009) in their studies with lipase (lipozyme-TL) immobilization from *Thermomyces lanuginosa* on aldehyde-funcionalized-APTS magnetic Fe_3O_4 nanoparticles.

Effect of the Contact Time

The effect of contact time was investigated and, as shown in Figure 3(C), the equilibrium enzyme-support interaction was quickly achieved at 1 h. During 4 hours, the amount of protein immobilized remained constant and the maximum derivative activity was observed. Only after 4 hours a decrease in catalytic activity was observed, possibly due to longer incubation time and conformational changes in the enzyme structure (Rodrigues *et al*., 2008).

Huang and Chen (2008) reported that a short contact time is required for enzyme immobilization on nanoparticles, due to the large surface area available, which reduces the resistance to mass transfer. Furthermore, the support modification with APTS and glutaraldehyde facilitated the rapid binding of the enzyme by covalent interactions between the aldehyde group of glutaraldehyde and the amine groups of the enzyme. A high concentration of aldehyde groups on the support surface may cause many multi-point covalent enzyme-support bonds, so as to obtain rigidity in the structure of the enzyme, favoring a high stability and a high intrinsic activity of the derivative (Betancor, *et al*., 2006).

Hu *et al*. (2009) reported that *Serratia marcescens* lipase was almost fully immobilized onto aldehyde-funcionalized-APTES magnetic nanoparticles within 10 min. Contact times up to 120 minutes did not show any significant change in the lipase immobilization, in agreement with those presented in this work.

Xie *et al*. (2009) also studied the influence of the immobilization time as a parameter on immobilization of lipase (lipozyme-TL) from *Thermomyces lanuginosa* on aldehyde-funcionalized-APTS magnetic nanoparticles Fe_3O_4 and reported that the optimum contact time was 2 h, with derivative activity maintenance for long time periods and profiles similar to the ones presented in Figure 3(C). These authors suggest that this behavior was due to the covalent enzyme

immobilization, where very long contact time provides multi-point binding and an excessive structural rigidity, making the enzyme inactive. Stronger multipoint binding thus seems to decrease the CALB-derivative activity; due to this, the activity recovery decreases, depending on the contact time. The results of Xie *et al*. (2009) also explain the catalytic activity decrease after 4 hours.

Figure 3(D) shows the consecutive hydrolysis cycles catalyzed by the different derivatives. The best results of hydrolytic activity after 6 cycles, approximately 50%, were obtained when the immobilization time was 1 h. Relative activities between 30-40% were achieved when the other derivatives, for which immobilization was carried out at different contact times, were used. Therefore, based on these results, all further biocatalysts were prepared with 1 hour for the contact time enzyme-support.

Functionalization Method and Biocatalyst Selection

Previous studies pointed to the effect of offered enzyme load in the immobilization reaction (50 to 200 $U.g^{-1}$). Immobilization reaction carried out with 200 $U.g^{-1}$ showed a higher final biocatalyst (MNPs/APTES) activity. However, the biocatalyst showed hydrolytic activity only when the immobilization reaction (carried out about 200 $U.g^{-1}$) occurred at neutral pH (pH = 7). No hydrolytic activity was observed when the immobilization reaction was carried out in basic medium (pH = 10). Based on these results, immobilization reactions were carried out at neutral pH.

The effect of the amount of amino groups on the immobilization of CALB (pH=7.0) was analyzed using magnetic derivatives obtained after 3–aminopropyltriethoxysilane functionalization at 1:1, 1:2 and 1:3 MNPs/APTES mass proportions.

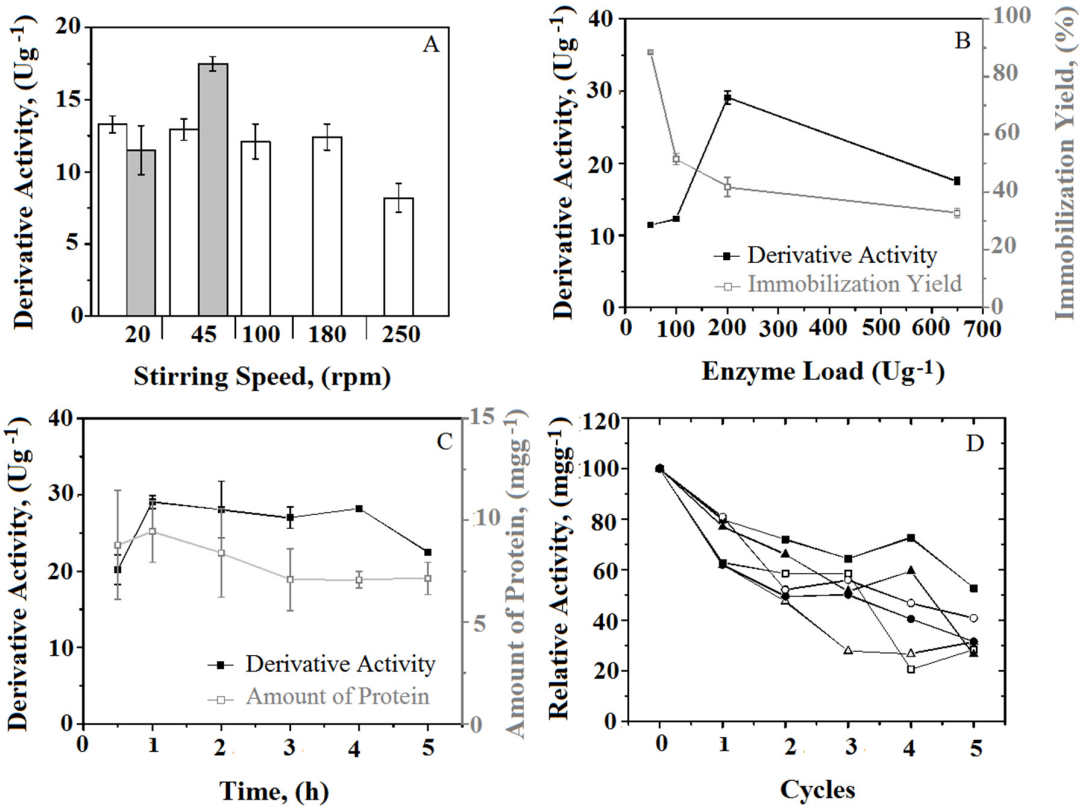

Figure 3: (A) Effect of stirring speed (rpm) on *Candida antactica Lipase B* (CALB) immobilization on magnetic nanoparticles (MNPs). 25 rpm and 45 rpm (rotational stirring, ■); 25 rpm, 45 rpm, 90 rpm, 180 rpm, 250 rpm (orbital stirring, □). **(B)** Effect of enzyme load on CALB immobilization on MNPs. Enzyme activity ($U.g^{-1}$) (■) and Immobilization yield (%) (□). The lines represent the trend of experimental data. **(C)** Effect of contact time on immobilization of CALB in MNPs. Enzyme activity ($U.\ g^{-1}$) (■) and amount of protein ($mg.\ g^{-1}$) (□). The lines represent the trend of experimental data. **(D)** Operational stability in the hydrolysis of p-nitrophenyl butyrate by CALB-MNPs derivatives. Relative activity (%): 30 min (□), 1 h (■), 2 h (Δ), 3 h (▲), 4 h (○), 5 h (●). The lines represent the trend of experimental data.

Table 1 shows that the immobilization yield and biocatalyst hydrolytic activity increased with APTES concentration on the nanoparticle. A greater silane amount adsorbed on the surface or a greater amount of amino groups present allow a greater number of active sites for crosslinking with glutaraldehyde and subsequently with CALB. Neutral pH (pH = 7) reaction facilitated linkages with non-catalytic enzyme regions, preserving the CALB active site and increasing the MNPs/APTES/CALB catalytic activity.

Table 1: Biocatalyst activity observed for derivatives obtained with different concentrations of 3-aminopropyl triethoxysilane (APTES) adsorbed on Magnétic Nanoparticles (MNPs).

Sample	Load (U)	Derivative Activity (U/g)	η (%)
NP/APTES 1:1	200	24.08	67.3
NP/APTES 1:2	200	25.11	69.7
NP/APTES 1:3	200	47.17	82.3

Biocatalyst Characterization

Figure 4 shows the diffraction pattern for the MNPs prepared by co-precipitation and functionalized with APTES (NP/APTES) in the ratio 1:3. This selected sample presents the best yield of functionalization. Crystallographic peaks and Miller indices found in the sample, which are reported in literature (Kim *et al*., 2012), were 21.4 ° (111), 35.2 ° (220), 41.6 ° (311), 50.7 ° (400) 63.2 ° (422), 67.5 ° (511) and 74.4 ° (440). These data are related to the cubic crystal system Fd-3m (227) space group that represents the characteristics of the unit cell of magnetite spinel, showing that the nanoparticles synthesized in this study are Fe_3O_4. Mathematical *Reitveld* refining treatment allowed calculating the crystallite size and particle size using the *Scherrer* method, resulting in 11 and 14.87 nm for MNPs and MNPs/APTES, respectively.

The first functionalization step, with APTES, aims to create a Si-O protective surface on the magnetic nanoparticles. As shown in the diffraction pattern for the NP/APTES, the peaks are slightly wider due to the formation of a Si-O layer, which gives it greater surface homogeneity. Functionalization increased the crystal NP/APTES nanocomposite organization degree (Feng *et al*., 2009; Valenzuela *et al*., 2009).

Figure 5 shows the FTIR spectra of the MNPs, MNPs/APTES(1:3) and MNPs/APTES(1:3)/CALB samples. The band at 582 cm^{-1} are related to the stretching of iron spinel bonds in the tetrahedral Fe site. The band at 1400 cm^{-1} is related to the angular bend vibration of Fe-O (Petcharoen and Sirivat, 2012). The band at 3410 cm^{-1} refers to stretching of OH bonds present in the nanoparticles due to their synthesis an aqueous medium and the presence of OH groups on the surface of the material (Can *et al*., 2009; Yamaura *et al*., 2004).

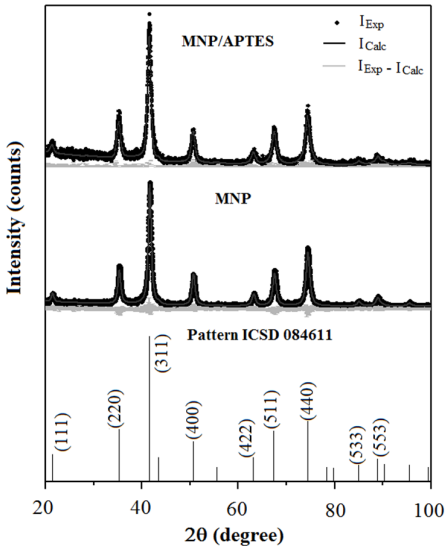

Figure 4: X-Ray Diffraction (DRX) pattern for the magnetic nanoparticles (MNPs) and MNPs after functionalization with 3-aminopropyl triethoxysilane (MNP/APTES) samples after the mathematical treatment of data by the *Reitveld* refining method.

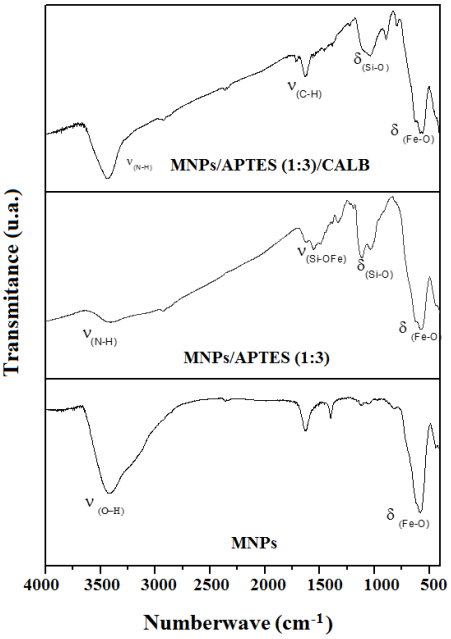

Figure 5: Fourier transform infrared spectroscopy (FTIR) of the magnetic nanoparticles (MNPs) and MNPs after functionalization with 3-aminopropyl triethoxysilane (APTES) and *Candida antarctica Lipase B* immobilized on MNP/APTES(1:3) (MNP/APTES(1:3)/ CALB).

Enzyme immobilization was observed in the MNPs/APTES 1:3/CALB FTIR spectra. The absorption bands at 1043 cm^{-1} and 1120cm^{-1} are attributed to the ν(Si-O) and Fe-Si, respectively. This result confirms the hypothesis presented for the diffraction pattern of NP/APTES, indicating a Fe_3O_4 nanoparticle surface coating after the APTES functionalization step. Besides Si-O signatures, the arrangement Si-O-Fe also possibly appears in the spectra. Bands for free amines on the material surface were found at 1629 cm^{-1} and 3424 cm^{-1}, which are due to N-H angular deformation and stretch (Bruce and Sen, 2005). The vibrational mode found at 1121 cm^{-1} is related to ν(C-N) bonds present in histidine and aspartate groups; the band for histidine groups at 795 cm^{-1} is relative to δ(HC = CH) out-of-the-plane vibration. The bands at 584-626 cm^{-1} appear in all systems, and refer to the tetrahedral δ(Fe-O) spinel iron bonds present in the magnetic phase.

The magnetization curves, shown in Figure 6, present the sample magnetization (M) in response to the applied magnetic field (H). A specific superparamagnetic behavior was observed for the nanoparticle sample. Coercivity characteristics and reminent magnetization equal to zero confirmed the magnetite superparamagnetic behavior (Goldman, 2006). The *Lagevin* function describes the magnetization curves for the samples (Auric *et al*., 1982), Equation (3):

$$M = N\mu^2 H / 3K_B T \quad (3)$$

where N, K_B, T, M, H and μ respectively indicate the number of Fe^{2+} ions, the Boltzmann constant, temperature, sample magnetization, external magnetic field and magnetic moment.

The particle size can also be inferred from this function via the *Lanvegin* parameter a (μ/K_B), which is related to the average particle diameter, since $a = 4\pi(d/2)3M_0/3K_B$, where d is the particle diameter. Average particle size from Langevin equation calculations results in 10 nm for MNPs and 13 nm for MNPs/APTES/CALB. This result is very close to the particle diameter obtained by the *Scherrer* method, confirming the particle size estimation accuracy. Based on these results a non-magnetic layer formation (3 nm), related to the functionalization, was evidenced. MNPs (Fe_3O_4) showed magnetic saturation (M_S) of 69 emu/g and, for the complete nanosystem (MNP/APTES/CALB). 35 emu/g. Thus, magnetization was observed even after the APTES functionalization step and surface CALB immobilization.

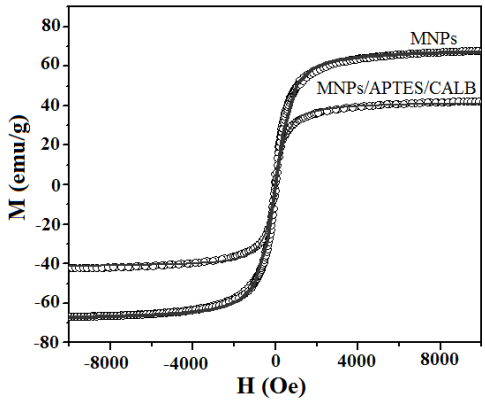

Figure 6: Magnetization curves for samples of magnetic nanoparticles (MNPs) and *Candida antarctica Lipase B* immobilized in MNPs after 3-aminopropyl triethoxysilane (APTES) functionalization and glutaraldehyde (GLU) reticulation (MNP/APTES/CALB).

These characterization results show that the effective APTES incorporation on the Fe_3O_4 nanoparticles created a suitable external layer upon CALB immobilization. This modification did not vary the cubic spinel structure of Fe_3O_4. Thus, immobilized lipase preserved the magnetic behavior, an important feature for the selective separation of immobilized enzymes.

Thermal Stabilities of Soluble and Immobilized CALB

The thermal stabilities of soluble and immobilized lipase were studied at 60 °C at pH 7.0 (25 mM sodium phosphate buffer) for 48 h. Figure 7 shows the inactivation for free and immobilized enzymes. The inactivation process is very fast for soluble CALB, which loses more than 70% of its initial activity in 6 minutes, while the immobilized one only exhibited a 20% loss of its initial activity. Even after 20 h, the immobilized lipase still retained 20% of its initial activity.

Table 2 shows the results of thermal deactivation at 60 °C of soluble CALB and CALB-NMP. For each thermal stability assay, the half-life ($t_{1/2}$) and the stabilization factor were determined. The half-life ($t_{1/2}$) increased from 3 to 60 minutes with the immobilization process. Immobilized enzyme was 20-fold more stable than the soluble enzyme at 60 °C. The enzyme in the soluble form presents some flexibility, which means that its active site undergoes conformational changes that are often irreversible, causing inactivity. When immobilized, a more rigid form is acquired because of linkages to the support. This stiffness decreases the flexibility of the enzyme, keeping the form of the active site, which is responsible for its

activity. The stabilization effects of the immobilization process with APTS and glutaraldehyde modification may be a consequence of both intermolecular crosslinks and intramolecular modifications (Fernandez-Lafuente *et al*., 1998).

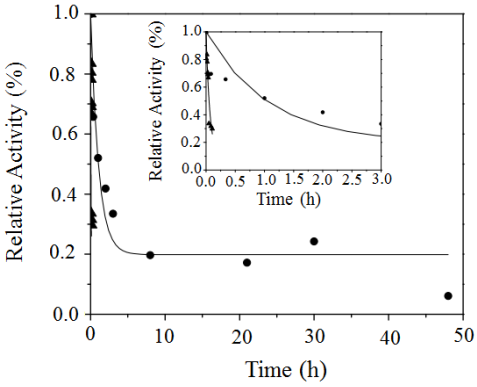

Figure 7: Thermal stability of free *Candida antarctica Lipase B* (CALB) and *Candida antarctica Lipase B* immobilized on MNPs after 3-aminopropyl triethoxysilane (APTES) functionalization and glutaraldehyde (GLU) reticulation at 60 °C and pH 7. Soluble enzyme At_i= 93 U.mL^{-1}. and CALB-MNPs At_t= 80 U.g^{-1}. Relative activity: immobilized CALB (●) and CALB free (▲). The lines represent the trend of the Sadana and Henley model.

Table 2: Thermal stability and thermal deactivation parameters at 60 °C for soluble *Candida antarctica* lipase B (CALB) and CALB-Magnetic Nanoparticles (biocatalyst) obtained after treatment with 3-aminopropyl triethoxysilane (APTES).

Biocatalyst	$Kd(h^{-1})$	$t_{1/2}(h)$	Stabilization factor (SF)
Soluble CALB	15.3	0.051	-
CALB/APTES/MNPs	0.94	1.0	20.0

Silva *et al*. (2012) showed the thermal deactivation at 60 °C of soluble CALB and CALB-Chitosan modified by different methods. The half-life of derivatives was found to be 1-3.3 h, with the immobilized enzyme being 12-33 times more stable than the soluble form. Hu *et al*. (2009) studied the effect of temperature on free and immobilized lipase (on aldehyde-functionalized magnetic Fe_3O_4 nanoparticles). The maximum activities of free and immobilized lipase were observed at 50 °C and 45 °C, respectively, but the immobilized lipase was more stable at higher temperatures (between 45 °C and 55 °C), in agreement with the data obtained in this work.

The MNPs/APTES/CALB operational stability was also observed at the end of each *p*NPB hydrolysis batch. The hydrolytic activity of the catalyst remained for 13 cycles. Only after 14 cycles was the catalyst activity reduced to 25% of its original/initial activity. Xie and Ma (2010) and Foresti and Ferreira (2005) showed stability studies for immobilized lipase on Fe_3O_4 nanoparticles and on polypropylene powder, respectively. Both Xie and Ma (2010) and Foresti and Ferreira (2005) pointed out that the stability of the biocatalyst obtained in their work remained for an average of 3-5 cycles. Thus, we can conclude that the process presented in this paper to obtain NPM/APTES/CALB showed better results when compared to Xie and Ma (2010) and Foresti and Ferreira (2005).

Hydrazinolytic Activity Analysis

Hydrazinolytic activity (HA) analyses (Figure 8) were performed to understand the INH synthesis performance.

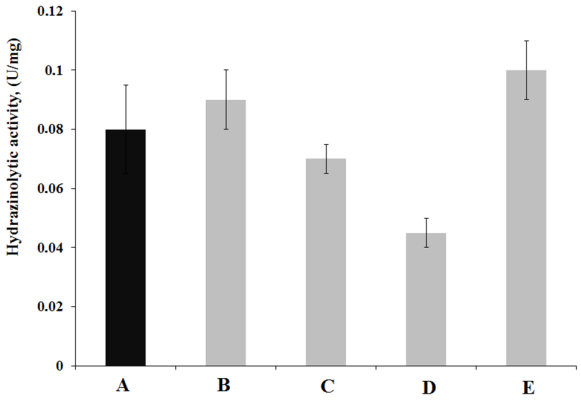

Figure 8: Hydrazinolytic activity for (A) NPMs/APTES/CALB, (B) OCSIL/CALB, (C) CHI/ CALB, (D) CHI/RML, and (E) commercial standard CALB L4777-3G® derivatives.

The results obtained for NPMs/APTES/CALB were 0.08 (± 0.015) U/mg. This value is very close to the values obtained by Honorato *et al*. (2013) using CHI/CALB biocatalyst (0.07 U/mg) and commercial standard Novozym 435. Similarly, hydrophobic supports offer good performance in organic reactions, as shown by the OCSIL/CALB performance.

Systems using *Rhizhomucor miehei* lipase (CHI/RML) presented lower results than other results (0.045 U/mg). The theoretical investigation of the dynamics of the *Rhizhomucor miehei* lipase active site showed the existence of alpha-helical *lid* structure in the catalytic cavity. The partial open conformation in the enzyme *lid* may have caused the worse results.

INH Synthesis

Figure 9 shows the ethyl isonicotinate (INE) conversion to INH by the hydrazinolysis reaction catalyzed by the tested biocatalysts. The results showed that the maximum MNPs/APTES(1:3)/CALB conversion is close to 18%. This result is similar to the OCSIL/CALB system. Novozym 435 commercial lipase (Sigma) immobilized on acrylic resin showed values close to 25% in 10 h of assay. Yadav *et al*. (2005), studying INH synthesis under similar conditions to those tested in these assays, reported similar values of INE conversion when the enzyme used was Novozym 435. Reaction with no catalyst presented conversion values (12h) close to 3-5%, consistent with Yadav *et al*. (2005).

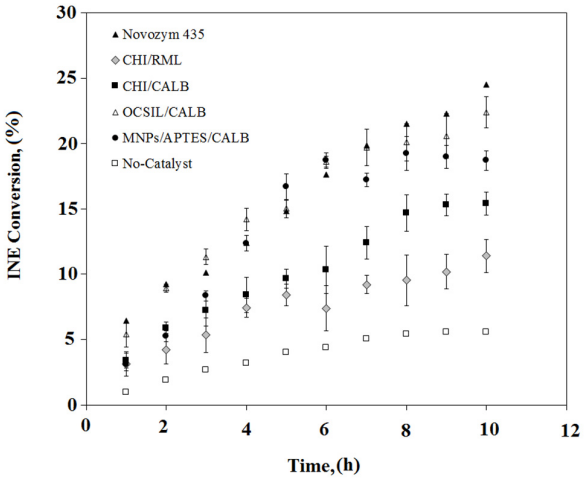

Figure 9: Ethyl isonicotinate (INE) conversion profiles for the isoniazide (INH) synthesis reaction catalyzed by *Candida antarctica Lipase B* immobilized on magnetic nanoparticles (NPMs/APTES(1:3)/CALB) (●), in chitosan-based (CHI/CALB) derivatives (■), on Octilsilane (OCSIL/CALB) derivatives (Δ), *Rhizomucor miehe Lipase* immobilized on chitosan-based derivatives (CHI/RML) (♦), *Candida antarctica Lipase B* commercial standard Novozym 435 (▲) and the catalyst-free reaction (□).

In comparison, the biocatalysts tested by Honorato *et al*. (2013) with chitosan-based supports presented lower values than those obtained for MNPs/APTES(1:3)/CALB. The results obtained by Honorato *et al*. (2013) indicate maximum INE conversions using CHI/RML and CHI/CALB of 10.2% (± 1.30) and 15.3% (± 0.81), respectively. These results suggested that the reduced performance of CHI/CALB and CHI/RML may be related to the structural changes caused by the chitosan-based support swelling during the INH synthesis reaction.

CONCLUSIONS

In general, CALB immobilized on glutaraldehyde-activated MNPs/APTES showed significant advantages over free enzyme. Temperature and operational stability of the immobilized enzyme were much better than those of the free enzyme. The biocatalyst recovery at the end of its use is very simple via low-cost magnetic processes. The co-precipitation chemical synthesis pathway is a low-cost and efficient route to NPMs with a good crystalline phase and controlled size and homogeneity. MNPs/APTES modification prepares the superparamagnetic nanostructures for multipoint CALB immobilization. The MNPs/APTES(1:3)/CALB biocatalyst provided the best hydrolytic activity results and this derivative was chosen for the INH synthesis tests. The INH synthesis results and the hydrazinolytic activity analysis allow the conclusion that the INE conversion profile is similar to reactions biocatalyzed by MNPs/APTES(1:3)/CALB, OCSIL/CALB and Novozym 435 derivatives. RML and CALB immobilized on non-conventional, low-cost, chitosan-based supports provided lower results for INH synthesis. Moreover, the INE synthesis biocatalyzed by MNPs/APTES(1:3)/CALB is a cyanopyridine-free process, conducted at mild temperatures with lower energy consumption. This makes the biocatalyzed synthesis process more attractive than the conventional chemical route for Industrial/large-scale applications.

ACKNOWLEDGMENTS

The authors would like to thank the Brazilian research-funding agencies FUNCAP, CNPq and CAPES for the financial support.

REFERENCES

Abbas, H. and Comeau, L., Aroma synthesis by immobilized lipase from *Mucor* sp. Enzyme and Microbial Technology, 32(5), 589-595 (2003).

Adachi, G. and Imanaka, N., The Binary Rare Earth Oxides. Chemical Reviews-American Chemical Society, 98, 1479-1514 (1998).

Adriano, W. S., Filho, E. H. C., Silva, J. A., Giordano, R. L. C. and Gonçalves, L. R. B., Stabilization of penicillin- G acylase by immobilization on

glutaraldehyde-activated chitosan. Brazilian Journal of Chemical Engineering, 22(4), 529-538 (2005).

Akoh, C., Chang, S., Lee, G. and Shaw, J., Enzymatic approach to biodiesel production. Journal of Agricultural and Food Chemistry, 55(22), 8995-9005 (2007).

Al-Zuhair, S., Ling, F. and Jun, L., Proposed kinetic mechanism of the production of biodiesel from palm oil using lipase. Process Biochemistry, 42(6), 951-960 (2007).

Auric, P., Dang, N. V., Bandyopadhyay, A. K. and Zarzycki, J., Superparamagnetism and ferrimagnetism of the small particles of magnetite in a silicate matrix. Journal of Non-Crystalline Solids, 50(1), 97-106 (1982).

Barreto, A. C. H., Maia, F. J. N., Santiago, V. R., Ribeiro, V. G. P., Denardin, J. C., Mele, G., Carbone, L., Lomonaco, D., Mazzetto, S. E. and Fechine, P. B. A., Novel ferrofluids coated with a renewable material obtained from cashew nut shell liquid. Microfluidics Nanofluidics, 12(5), 677-686 (2011).

Barry, C. E., New horizons in the treatment of tuberculosis. Biochemical Pharmacology, 54(11), 1165-1172 (1997).

Betancor, L., López-Gallego, F., Hidalgo, A., Alonso-Morales, N., Mateo, G. D. O., Fernàndez-Lafuente, R., and Guisàn, J. M., Different mechanisms of protein immobilization on glutaraldehyde activated supports: Effect of support activation and immobilization conditions. Enzyme and Microbial Technology, 39(4), 877-882 (2006).

Björkling, F., Godtredsen, S. and Kirk, O., The future impact of industrial lipases. Trends in Biotechnology, 9(1), 360-363 (1991).

Bruce, I. J. and Sen, T., Surface modification of magnetic nanoparticles with alkoxysilanes and their application in magnetic bioseparations. Langmuir, 21(15), 7029-7035 (2005).

Brzozowsky, A. M., Derewenda, U., Derewenda, Z. S., Dodson, G. G., Lowson, D. M. and Turkenburg, J. P., A model for interfacial activation in lipases from the structure of a fungal lipase inhibitor complex, Nature, 351(6326), 491-4 (1991).

Can, K., Ozmen, M. and Ersoz, M., Immobilization of albumin on aminosilane modified superparamagnetic magnetite nanoparticles and its characterization. Colloids and Surfaces B: Biointerfaces, 71(1), 154-159 (2009).

Feng, B., Hong, R. Y., Wang, L. S., Guo, L., Li, H. Z., Ding, J., Zheng, Y. and Wei, D. G., Synthesis of Fe_3O_4/APTES/PEG diacid functionalized magnetic nanoparticles for MR imaging. Colloids and Surfaces A: Physicochemical and Engineering Aspects, 328(1-3), 52-59 (2008).

Fernandez-Lafuente, R., Rosell, C., Rodriguez, V., Santana, C., Soler, G., Bastida, A. and Guisan, J., Preparation of activated supports containing low pK amino groups. A new tool for protein immobilization via the carboxyl coupling method. Enzyme and Microbial Technology, 15(7), 546-550 (1993).

Foresti, M. and Ferreira, M., Solvent-free ethyl oleate synthesis mediated by lipase from *Candida antarctica B* adsorbed on polypropylene powder. Catalysis Today, 107-108, 23-30 (2005).

Gogte, V. N., Profiles in Drug Syntheses. Gokul Publishers, Bombay, India (1982).

Goldman, A., Modern Ferrite Technology. Springer US, New York (2006).

Gotor, V., Brieva, R., Gonzalez, C. and Rebolledo, F., Enzymatic aminolysis and transamidation reaction. Tetrahedron, 47(44), 9207-9214 (1991).

Gotor-Fernández, V., Busto, E. and Gotor, V., *Candida antarctica* lipase B: An ideal biocatalyst for the preparation of nitrogenated organic compounds. Advanced Synthesis and Catalysis, 348(7-8), 797-812 (2006).

Hæffner, F., Norin, T. and Hult, K., Molecular modeling of the enantioselectivity in lipase-catalyzed transesterification reactions. Biophysical Journal, 74(3), 1251-1262 (1998).

Honorato, T. L., Macedo, A. C. and Gonçalves, L. R. B., Produção de isoniazida utilizando lipase imobilizada em quitosana. XIX Simpósio Nacional de Bioprocessos, Foz do Iguaçú, Anais do XV Simpósio Nacional de Bioprocessos (2012). (In Portuguese).

Hu, B., Pan, J., Yu, H., Liu, J. and Xu, J., Immobilization of *Serratia marcescens* lipase onto amino-functionalized magnetic nanoparticles for repeated use in enzymatic synthesis of Diltiazem intermediate. Process Biochemistry, 44(9), 1019-1024 (2009).

Huang, L., and Cheng, Z., Immobilization of lipase on chemically modified bimodal ceramic foams for olive oil hydrolysis. Chemical Engineering Journal, 144(1), 103-109 (2008).

Jang, J. H. and Lim, H. B., Characterization and analytical application of surface modified magnetic nanoparticles. Microchemical Journal, 94(2), 148-158 (2010).

Kaya, F., Heitmann, J. and Joyce, T., Cellulase binding to cellulose fibers in high shear fields. Journal of Biotechnology, 36(1), 1-10 (1994).

Kim, H., Youn, S., and Shin, C., Lipase-catalyzed synthesis of sorbitol – fatty acid esters at extremely

high substrate concentrations. Journal of Biotechnology, 123(2), 174-184 (2006).

Kim, W., Suh, C., Cho, S., Roh, K., Kwon, H., Song, K. and Shon, I., A new method for the identification and quantification of magnetite – maghemite mixture using conventional X-ray diffraction technique. Talanta, 94, 348-352 (2012).

Kordel, M., Hofmann, B., Schomburg, D. and Schmid, R., Extracellular lipase of *Pseudomonas sp*. strain ATCC 21808: Purification, characterization, crystallization, and preliminary X-ray diffraction data. Journal of Bacteriology, 173(15), 4836-4841 (1991).

Lei, L., Bai, Y., Li, Y., Yi, L., Yang, Y. and Xia, C., Study on immobilization of lipase onto magnetic microspheres with epoxy groups. Journal of Magnetism and Magnetic Materials, 321(4), 252-258 (2009).

Lima de Matos, L. J. B., Síntese de Biodiesel por Transesterificação Enzimática Empregando Lipases Imobilizadas e Estabilizadas. PhD Thesis, Universidade Federal do Ceará (2014). (In Portuguese).

López-Gallego, F., Betancor, L., Mateo, C., Hidalgo, A., Alonso-Morales, N., Dellamora-Ortiz, G. and Fernàndez-Lafuente, R., Enzyme stabilization by glutaraldehyde crosslinking of adsorbed proteins on aminated supports. Journal of Biotechnology, 119(1), 70-75 (2005).

Matei, L., Bleotu, C., Baciu, I., Draghici, C., Ionita, P., Paun, A., Chifiriuc, M. C., Sbarcea, A. and Zarafu, I., Synthesis and bioevaluation of some new isoniazid derivatives. Bioorganic and Medicinal Chemistry, 21(17), 5355-5361 (2013).

Mendes, A. A., Oliveira, P. C., Vèlez, A. M., Giordano, R. L. C., Giordano, R. C. and Castro, H. F., Evaluation of immobilized lipases on poly-hydroxybutyrate beads to catalyze biodiesel synthesis. International Journal of Biological Macromolecules, 50(3), 503-511 (2012).

Mohy Eldin, M. S., Schroen, C. G. P. H., Janssen, A. E. M., Mita, D. G. and Tramper, J., Immobilization of Penicillin G acylase on chemically grafted nylon particles. Journal of Molecular Catalysis B: Enzymatic, 10(4), 445-451 (2000).

Mozhaev, V. and Martinek, K., Inactivation and reactivation of proteins (enzymes). Enzyme and Microbial Technology, 4(5), 299-309 (1982).

Rodrigues, D. S., Mendes, A. A., Adriano, W., Gonçalves, L. R. B. and Giordano, R. L. C., Multipoint covalent immobilization of microbial lipase on chitosan and agarose activated by different methods. Journal of Molecular Catalysis B: Enzymatic, 51(3), 100-109 (2008).

Sadana, A. and Henley, J. P., Single-step unimolecular non-first-order enzyme deactivation kinetics. Biotechnology and Bioengineering, 30(6), 717-723 (1987).

Sadana, A., Enzyme deactivation. Biotechnology Advances, 6(3), 349-446 (1988).

Silva, J. A., Macedo, G. P., Rodrigues, D. S., Giordano, R. L. C. and Gonçalves, L. R. B., Immobilization of *Candida antarctica* lipase B by covalent attachment on chitosan-based hydrogels using different support activation strategies. Biochemical Engineering Journal, 60, 16-24 (2012).

Sittig, M., Pharmaceutical Manufacturing Encyclopedia. 2nd (Ed.), Noyes Publications, New Jersey-USA (1988).

Tani, K. and Suzuki, Y., Influence of titania matrix on retention behaviour in reversed-phase liquid chromatography. J. Chromatography A, 722(1), 129- 134 (1996).

Valenzuela, R., Fuentes, M. C., Parra, C., Baeza, J. Duran, N., Sharma, S. K., Knobel, M. and Freer, J., Influence of stirring velocity on the synthesis of magnetite nanoparticles (Fe_3O_4) by the co-precipitation method. Journal of Alloys and Compounds, 488(1), 227-231 (2009).

Vavříková, E., Polanc, S., Kočevar, M., Košmrlj, J., Horváti, K., Bősze, S., Stolaříková, J., Imramovský, A. and Vinšová, J., New series of isoniazid hydrazones linked with electron-withdrawing substituents. European Journal of Medicinal Chemistry, 46(12), 5902-5909 (2011).

World Health Organization, Global Tuberculosis Report 2014, WHO Library (2014).

Xie, W. and Ma, N., Immobilized lipase on Fe_3O_4 nanoparticles as biocatalyst for biodiesel production. Energy and Fuels, 23(3), 1347-1353 (2009).

Yadav, G. D. and Sajgure, A. D., Synergism of microwave irradiation and enzyme catalysis in synthesis of isoniazid. Journal of Chemical Technology and Biotechnology, 82(11), 964-970 (2007).

Yadav, G. D., Joshi, S. S. and Lathi, P. S., Enzymatic synthesis of isoniazid in non-aqueous medium. Enzyme and Microbial Technology, 36(2-3), 217-222 (2005).

Yesiloglu, Y., Utilization of bentonite as a support material for immobilization of *Candida rugosa* lipase. Process Biochemistry, 40(6), 2155-2159 (2005).

Yong, Y., Bai, Y., Li, Y., Lin, L., Cui, Y. and Xia, C., Characterization of *Candida rugosa* lipase immobilized onto magnetic microspheres with hydrophilicity. Process Biochemistry, 43(11), 1179-1185 (2008).